

ON THE ORIGIN OF THE COLOR-MAGNITUDE RELATION IN THE VIRGO CLUSTER

ALEXANDRE VAZDEKIS,^{1,2} HARALD KUNTSCHNER,¹ ROGER L. DAVIES,¹ NOBUO ARIMOTO,³
OSAMU NAKAMURA,³ AND REYNIER PELETIER⁴

Received 2000 October 17; accepted 2001 March 13; published 2001 April 13

ABSTRACT

We explore the origin of the color-magnitude relation (CMR) of early-type galaxies in the Virgo Cluster using spectra of very high signal-to-noise ratio for six elliptical galaxies selected along the CMR. The data are analyzed using a new evolutionary stellar population synthesis model to generate galaxy spectra at the resolution given by their velocity dispersions. In particular, we use a new age indicator that is virtually free of the effects of metallicity. We find that the luminosity-weighted mean ages of Virgo ellipticals are greater than ~ 8 Gyr and show no clear trend with galaxy luminosity. We also find a positive correlation of metallicity with luminosity, color, and velocity dispersion. We conclude that the CMR is driven primarily by a luminosity-metallicity correlation. However, not all elements increase equally with the total metallicity, and we speculate that the CMR may be driven by both a total metallicity increase and a systematic departure from solar abundance ratios of some elements along the CMR. A full understanding of the role played by the total metallicity, abundance ratios, and age in generating the CMR requires the analysis of spectra of very high quality, such as those reported here, for a larger number of galaxies in Virgo and other clusters.

Subject headings: galaxies: abundances — galaxies: clusters: general —
galaxies: clusters: individual (Virgo) — galaxies: elliptical and lenticular, cD —
galaxies: evolution — galaxies: stellar content

1. INTRODUCTION

To understand how galaxies form and evolve, we need to account for the *color-magnitude relation* (CMR): luminous early-type galaxies in clusters are observed to be redder than fainter ones (Visvanathan & Sandage 1977; Bower, Lucey, & Ellis 1992a). This tight relation, together with the related M_{g_2} - σ relation (Colless et al. 1999), links the mass of a galaxy, through its luminosity, to its constituent stellar populations.

The origin of the CMR is hotly debated: it could be caused either by a variation of the mean stellar metallicity along the sequence (Arimoto & Yoshii 1987; Kodama & Arimoto 1997) or by a combination of age *and* metallicity variations (González 1993; Ferreras, Charlot, & Silk 1999). Larson (1974) suggested a dissipational collapse picture for the formation of ellipticals with an early formation of the bulk of the stars. In this scenario more luminous galaxies have greater binding energies and can therefore achieve higher metallicities. Terlevich et al. (1999) provided support for this view by showing that the Coma Cluster galaxies on the CMR are old and that the galaxies with bluer colors than expected for their luminosity are younger. In more complex star formation histories, such as implied by hierarchical merging (Cole et al. 1994; Kauffmann & Charlot 1998) where galaxies have some recent star formation due to late merger events, the CMR might be expected to arise from a combination of age and metallicity variations. Indeed, González (1993), Jørgensen (1999), and Trager et al. (2000a) find strong evidence for a significant intermediate-age population in some elliptical galaxies. Trager et al. (2000b) reported a large age range in their

full sample but note that the galaxies in clusters are generally old. They also find a tight age–metallicity–velocity dispersion relation such that, at a fixed velocity dispersion, metal-rich galaxies are young and conjecture that this relation might give rise to a tight CMR.

Broadband colors and line strength indices of integrated stellar populations are sensitive to changes in both age *and* metallicity, and this degeneracy has prevented an unambiguous analysis of the ages and metallicities of ellipticals along the CMR (Worthey 1994). Even the widely used age indicator in the Lick/IDS system, $H\beta$, shows a nonnegligible dependence on metallicity (Worthey 1994) and can be affected by emission (Davies, Sadler, & Peletier 1993; González 1993). The origin of the CMR is not yet fully understood, in part, because of the lack of appropriate tools of analysis.

In this Letter we study the stellar populations of six Virgo ellipticals selected along the CMR for which we have very high signal-to-noise ratio (S/N) spectra. We use a new stellar population synthesis model in combination with new, more sensitive age indicators to derive age estimates that are virtually independent of the metallicity.

2. STELLAR POPULATION MODELS

Here we use the evolutionary stellar population synthesis model of Vazdekis (1999), which employs the extensive empirical stellar spectral library of Jones (1999). The model predicts spectral energy distributions (SEDs) in the optical wavelength range for simple stellar populations at a resolution of 1.8 \AA (FWHM). Previous models (e.g., Worthey 1994; Vazdekis et al. 1996) used mostly the Lick polynomial fitting functions (Worthey et al. 1994; Worthey & Ottaviani 1997) to relate the strengths of selected absorption features to stellar atmospheric parameters. The fitting functions are based on the Lick/IDS stellar library (FWHM $\sim 9 \text{ \AA}$; Worthey et al. 1994), thus limiting the application of the models to strong features. Furthermore, the Lick stellar library has not been flux-calibrated,

¹ Department of Physics, University of Durham, South Road, Durham DH1 3LE, UK; vazdekis@ll.iac.es, harald.kuntschner@durham.ac.uk, roger.davies@durham.ac.uk.

² Instituto de Astrofísica de Canarias, Vía Láctea s/n, E-38200 La Laguna, Tenerife, Spain.

³ Institute of Astronomy, University of Tokyo, Osawa 2-21-1, Mitaka, Tokyo 181-0015, Japan; arimoto@ioa.s.u-tokyo.ac.jp, nakamura@ioa.s.u-tokyo.ac.jp.

⁴ School of Physics and Astronomy, University of Nottingham, University Park, Nottingham, NG7 2RD, UK; reynier.peletier@nottingham.ac.uk.

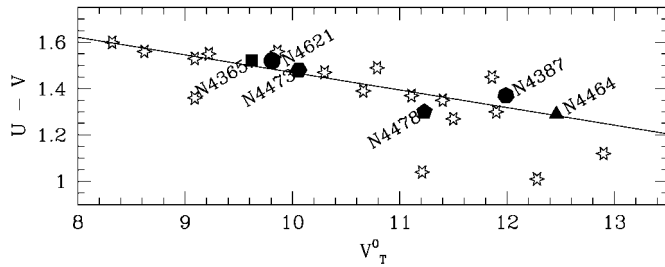


FIG. 1.—CMR in the Virgo Cluster. Data and a best-fit regression (ellipticals only) from Bower et al. (1992a, 1992b). For NGC 4464 we have taken V_T from de Vaucouleurs et al. (1991, hereafter RC3). For NGC 4478 we used Michard (1982) $U-V$ color ($60''$ aperture), applying an offset of -0.047 , obtained by a comparison of his nonreddened $U-V$ colors with those of Bower et al. (1992b), which are dereddened by -0.02 . Filled symbols represent our sample of galaxies; the shapes are used to identify the six galaxies in the following figures.

so offsets had to be applied to data obtained with different spectrographs (Worthey & Ottaviani 1997).

The new model provides flux-calibrated, high-resolution spectra, therefore allowing an analysis of galaxy spectra at the natural resolution given by their internal velocity broadening and instrumental resolution. Furthermore, as the model outputs are SEDs rather than predicted index strengths, it is easy to define new indices and even to confront the model predictions with the detailed structure of observed absorption features. Vazdekis & Arimoto (1999) defined a new age indicator $[\text{H}\gamma + \frac{1}{2}(\text{Fe I} + \text{Mg I})]_0$ (hereafter $\text{H}\gamma_0$), which is virtually free from metallicity dependence. To cover a large range in σ , Vazdekis & Arimoto defined three slightly different indices that give stable and sensitive age predictions within the σ ranges quoted in the subindices: $\text{H}\gamma_{100 < \sigma < 175}$, $\text{H}\gamma_{150 < \sigma < 225}$, and $\text{H}\gamma_{225 < \sigma < 300}$.

We emphasize that the model spectra we are fitting have a single metallicity and age. We are measuring luminosity-weighted properties, which means that the presence of a young (i.e., bright) stellar component will disproportionately affect the mean age and therefore will be detected more easily.

3. DATA

We obtained major axis spectra of very high S/N for six Virgo ellipticals, NGC 4365, NGC 4387, NGC 4464, NGC 4473, NGC 4478, and NGC 4621, selected along the CMR of Bower, Lucey, & Ellis (1992a, 1992b) (see Fig. 1 and also Table 1). The observations were performed at the William Herschel Telescope (4.2 m) at the Observatorio del Roque de Los Muchachos, La Palma, on 1999 April 21–22. We used the ISIS double-beam spectrograph with the EEV12 CCD and R600B grating in the blue channel, which provided a dispersion of $0.44 \text{ \AA pixel}^{-1}$ and a spectral range of $\lambda\lambda \sim 4000\text{--}5500 \text{ \AA}$. The slit width was set to $1''.6$, giving a spectral resolution of 2.4 \AA (FWHM). The seeing was $2''\text{--}3''$ in the first night and $\sim 1''.5$ in the second. The CCD was binned times 3 in the spatial direction giving $0''.57$ per bin. Multiple exposures of 35 minutes length were obtained for each galaxy.

Data reduction was done with standard IRAF packages. We made use of tungsten flat fields obtained for each galaxy pointing. The continuum shape was corrected to a relative flux scale with spectrophotometric standards.

We summed up the spectra within $r_e/10$, where effective radii were taken from Burstein et al. (1987). Before summation the central galaxy spectra were carefully aligned with the rows of the array, and each row in spatial direction was corrected for the velocity shift due to rotation. Variations of σ within $r_e/10$

TABLE 1
VIRGO GALAXY SAMPLE

Galaxy	Exposure (minutes)	$r_e/10$	S/N per \AA	σ (km s^{-1})	V_T^0 ^a	$(U-V)_{10}^0$ ^b
NGC 4464	105	0''.6	~ 160	~ 135	12.46 ^c	1.46 ^a
NGC 4387	105	2''.6	~ 130	~ 105	11.99	1.50
NGC 4478	105	1''.7	~ 135	~ 135	11.23	1.50
NGC 4473	70	2''.7	~ 280	~ 180	10.06	1.61
NGC 4621	140	6''.0	~ 490	~ 230	9.81	1.64
NGC 4365	70	6''.7	~ 250	~ 255	9.62	1.67

^a Bower et al. 1992b.

^b Michard 1982. $(U-V)_{10}^0$ corrected to $r_e/10$ from $(U-V)_e$ using the mean gradient of Trager et al. 2000b. Galactic extinction corrected using Schlegel, Finkbeiner, & Davis 1998.

^c RC3.

were small ($< 25 \text{ km s}^{-1}$) for all galaxies, and therefore no correction was applied. Table 1 lists the S/N per angstrom unit achieved in the summed spectra around the $\text{H}\gamma$ feature.

4. THE AGES AND METALLICITIES OF VIRGO ELLIPTICALS

In this section we (1) compare the sensitivity and precision of different age indicators, (2) demonstrate that not all metals are enhanced at the same rate in more luminous (higher dispersion) galaxies, and (3) show that for the six Virgo ellipticals studied here metallicity increases with luminosity, velocity dispersion, and color but no trend with age is apparent.

Our primary goal is to measure the ages of the central regions of the galaxy sample along the CMR. We use different age indicators: $\text{H}\gamma_0$, $\text{H}\delta_F$, and $\text{H}\beta$ (as defined by Vazdekis & Arimoto 1999, Worthey & Ottaviani 1997, and Worthey et al. 1994, respectively). Instead of applying σ corrections to the line-strength measurements, we modified the model predictions. We divided our sample into three groups containing galaxies with similar velocity dispersions and smoothed the SEDs of Vazdekis (1999) accordingly. We chose (1) $\sigma_{\text{tot}} = 145$, (2) $\sigma_{\text{tot}} = 190$, and (3) $\sigma_{\text{tot}} = 260 \text{ km s}^{-1}$ (where $\sigma_{\text{tot}}^2 = \sigma_{\text{galaxy}}^2 + \sigma_{\text{instr.}}^2$). To minimize the effect of small velocity dispersion differences, the spectrum of NGC 4387 was convolved with a Gaussian of $\sigma = 85 \text{ km s}^{-1}$ and that of NGC 4621 with $\sigma = 105 \text{ km s}^{-1}$.

Figure 2 shows age/metallicity diagnostic diagrams for the age indicators as a function of the mean metallicity indicator $[\text{MgFe}]$ (González 1993). Velocity dispersion increases in each column from top to bottom. Note that for a given age and metallicity the strength of the $[\text{MgFe}]$ index is smaller for larger σ . The left panels of Figure 2 show how well $\text{H}\gamma_0$ is able to break the age-metallicity degeneracy, much better than, e.g., $\text{H}\delta_F$. The lines of constant age are essentially horizontal, which means that a given measurement of $\text{H}\gamma_0$ corresponds to a unique age. $\text{H}\beta$ is also a good age indicator; the new models predict that $\text{H}\beta$ is more sensitive to age and less sensitive to metallicity than models using the Lick fitting functions.

Overall we find good agreement between the ages inferred from $\text{H}\gamma_0$ and $\text{H}\beta$. All our galaxies, except for NGC 4478, are older than ~ 11 Gyr. NGC 4478 is 8–9 Gyr old and has a $U-V$ color 0.06 mag bluer than other Virgo ellipticals of equivalent luminosities (see Fig. 1)

The middle panels of Figure 2 show that the age estimates based on $\text{H}\delta_F$ remain strongly coupled with metallicity estimates. (N.B. the $\text{H}\gamma_F$ index is similar and is not plotted.) The age estimates based on $\text{H}\delta_F$ are younger than those derived from $\text{H}\gamma_0$ or $\text{H}\beta$, but we are unable to distinguish between genuinely younger ages and the possible systematic effects of nonsolar abundance ratios. For example, using $\text{H}\delta_F$ or $\text{H}\gamma_F$ as

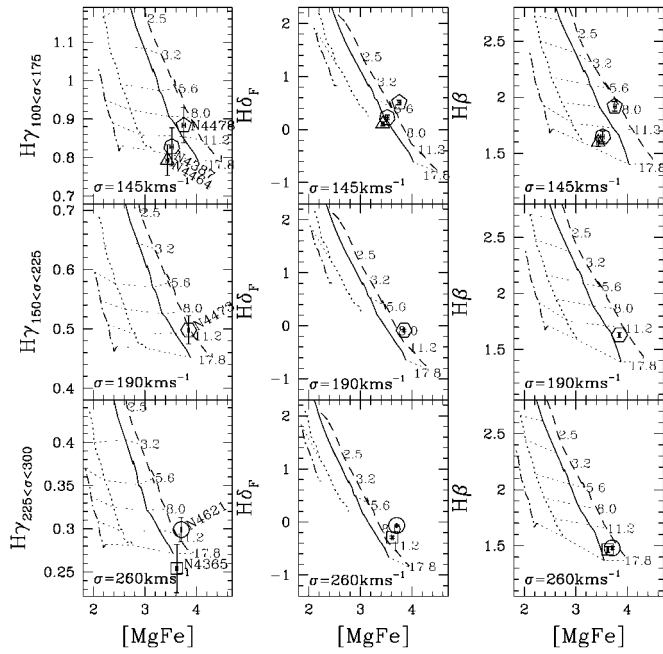


FIG. 2.—From left to right: Plots of $H\gamma_{\sigma}$, $H\delta_F$, and $H\beta$ vs. the metallicity index $[MgFe]$ (defined in González 1993). The central velocity dispersion increases in three groups from top to bottom, representing the CMR. Overplotted are the models by Vazdekis (1999). Lines of constant $[Fe/H] = -0.7, -0.4, 0.0,$ and 0.2 are shown by thick dot-dashed, thick dotted, thick solid, and thick dashed lines, respectively. Thin dotted lines represent models of constant ages, which are quoted in gigayears.

the age indicator, one derives younger ages when $Mg\ b$ and/or Mg_2 are used as the metal indicator than when the Fe lines alone are used (Worthey 1998; Kuntschner 2000).

Figure 3 plots the $H\gamma_{\sigma}$ indices against the strength of four metal absorption lines and illustrates the effects of nonsolar abundance ratios in determining metallicity. The left-hand columns in Figure 3 show only a very modest increase in the metallicity derived from $Fe3^5$ or $Ca4227$ as velocity dispersion increases from top to bottom. We note that the G band also follows $Fe3$. In contrast, the right-hand columns in Figure 3 show that the metallicity derived from $Mg\ b$ or $CN2$ increases significantly toward high velocity dispersion galaxies, extending beyond the model grids in some cases. Although Ca, like Mg, is an α -element, we find that $Ca4227$ does not track $Mg\ b$, confirming the results reported by Vazdekis et al. (1997), Worthey (1998), and Trager et al. (2000a). We conclude that there are at least two families of metal lines, which give rise to very different metallicity estimates and exhibit different trends along the CMR. Despite these complexities in estimating “metallicity,” we emphasize that by using $H\gamma_{\sigma}$ these uncertainties do not influence our derived ages.

Figure 4 shows our estimates for luminosity-weighted mean age and metallicity (derived from $H\gamma_{\sigma}$ and $H\beta$ versus $[MgFe]$ in Fig. 2) versus galaxy luminosity, color, and velocity dispersion. Except for NGC 4478, all ellipticals are old, with ages ranging from ~ 11 to ~ 20 Gyr. There is no trend in age along the CMR, but there is a clear, positive correlation of metallicity with V_T^0 , $U-V$, and σ . If we correct the metallicity estimates to the value they would have if all the galaxies were 14 Gyr old, the scatter in Figure 4 is reduced. Furthermore, our $[MgFe]$ index yields very similar metallicities to those derived by correcting the Fe indices for nonsolar abundance ratios, following

⁵ $Fe3 = \frac{1}{3}(Fe4383 + Fe5270 + Fe5335)$; Kuntschner (2000).

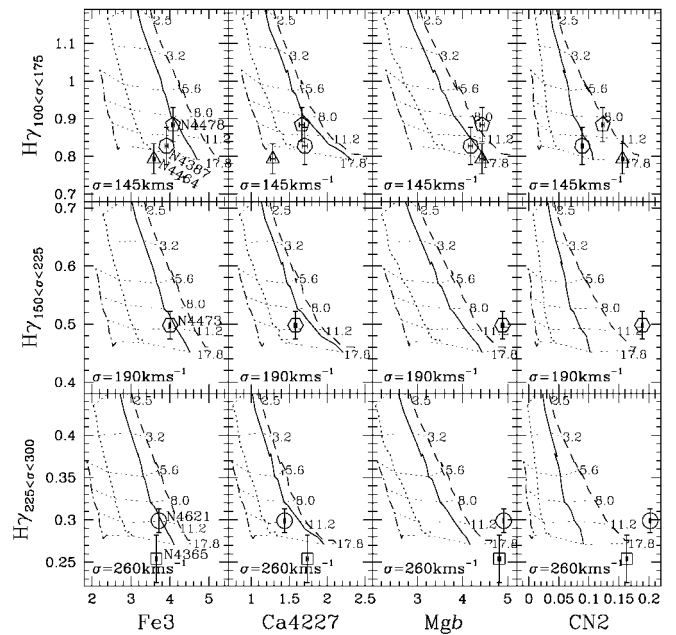


FIG. 3.—Plots of $H\gamma_{\sigma}$ vs. $Fe3$, $Mg\ b$, $Ca4227$, and $CN2$. Symbols and line styles are the same as in Fig. 2.

Trager et al. (2000a). We conclude that for these six galaxies in Virgo the metal content increases along the CMR.

5. CONCLUSIONS

We have performed a detailed spectral analysis of six elliptical galaxies in the Virgo Cluster. We have combined very high S/N spectra with a new evolutionary stellar population synthesis model. This model enables us to study galaxy spectra at the resolution given by their velocity dispersions and de-

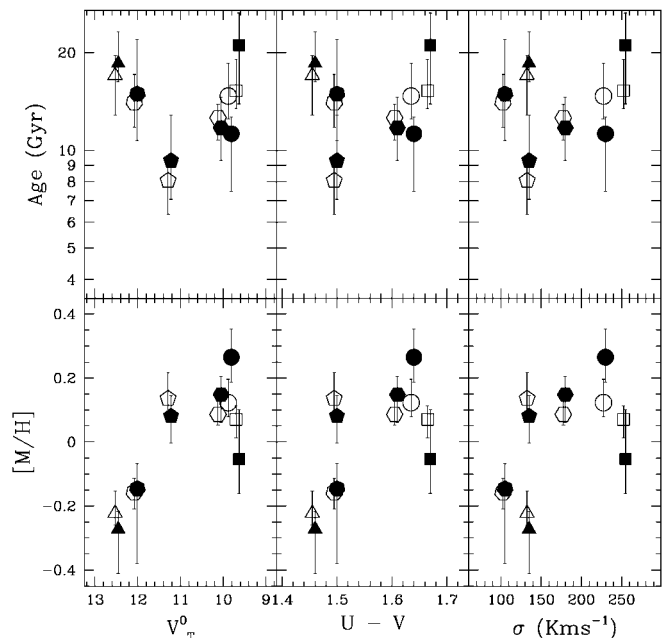


FIG. 4.—Mean galaxy ages and metallicities as estimated from $H\gamma_{\sigma}$ (filled symbols) and $H\beta$ (open symbols) (derived from $H\beta$ vs. $[MgFe]$ diagrams) vs. V_T^0 , $U-V$, and velocity dispersion. The error bars for the $H\gamma_{\sigma}$ age and metallicity estimates are mainly due to noise, while those for $H\beta$ are dominated by the larger age/metallicity degeneracy affecting this index.

termine ages that are virtually free of any dependence on metallicity. We find that elliptical galaxies in Virgo are generally old.

We find that the metallicity as measured by $[Mg/Fe]$ correlates with luminosity, $U-V$, and velocity dispersion. We conclude that the CMR in Virgo is driven primarily by an increase in metallicity with luminosity. We find that not all elements increase equally with the total metallicity estimates. For example, the increase in metallicity as measured from the Fe or Ca indices is very modest along the CMR, whereas the Mg or CN indices indicate a more rapid increase with galaxy luminosity. This is consistent with the findings of Worthey, Faber, & González (1992), Kuntschner (2000), and Trager et al. (2000b), who find an increase of the $[Mg/Fe]$ ratio with increasing central velocity dispersion. We speculate that the CMR in Virgo may be driven by both a total metallicity increase and a systematic departure from solar abundance ratios of some elements along the CMR.

The luminosity-weighted mean ages range from ~ 8 to 20 Gyr, but there is no clear trend between age and V_r^0 , $U-V$, or σ . Trager et al. (2000b) note that at a given velocity dispersion

galaxies with younger ages have higher metallicity. Our Virgo galaxies fall on the Trager dispersion-age-metallicity relation but span less than one-half the range of ages and metallicities that are found in their sample. Trager et al. suggest that the distribution of ages and metallicities among ellipticals may depend on environment, and indeed our Virgo galaxies exhibit a much smaller range than that found in their mixed-environment sample. We cannot determine whether the small age range we find here is universal in cluster ellipticals, but we intend to address this question in future work.

The authors thank J. Blakeslee, R. Bower, J. Gorgas, T. Kodama, J. Lucey, and the referee, J. J. González, for valuable discussions and suggestions. A. V. and H. K. acknowledge the support of the PPARC rolling grant “Extragalactic Astronomy and Cosmology in Durham 1998–2002.” This work was financially supported in part by a Grant-in-Aid for Scientific Research (1164032) by the Japanese Ministry of Education, Culture, Sports, and Science. R. L. D. acknowledges the support of a Leverhulme Trust Research Fellowship.

REFERENCES

- Arimoto, N., & Yoshii, Y. 1987, *A&A*, 173, 23
 Bower, R. G., Lucey, J. R., & Ellis, R. S. 1992a, *MNRAS*, 254, 601
 ———. 1992b, *MNRAS*, 254, 589
 Burstein, D., Davies, R., Dressler, A., Faber, S., Stone, R., Lynden-Bell, D., Terlevich, R., & Wegner, G. 1987, *ApJS*, 64, 601
 Cole, S., Aragon-Salamanca, A., Frenk, C. S., Navarro, J. F., & Zepf, S. E. 1994, *MNRAS*, 271, 781
 Colless, M., Burstein, D., Davies, R. L., McMahan, R., Saglia, R., & Wegner, G. 1999, *MNRAS*, 303, 813
 Davies, R. L., Sadler, E. M., & Peletier, R. F. 1993, *MNRAS*, 262, 650
 de Vaucouleurs, G., et al. 1991, *Third Reference Catalogue of Bright Galaxies* (New York: Springer) (RC3)
 Ferreras, I., Charlot, S., & Silk, J. 1999, *ApJ*, 521, 81
 González, J. J. 1993, Ph.D. thesis, Univ. California, Santa Cruz, Lick Obs.
 Jones, L. A. 1999, Ph.D. thesis, Univ. North Carolina, Chapel Hill
 Jørgensen, I. 1999, *MNRAS*, 306, 607
 Kauffmann, G., & Charlot, S. 1998, *MNRAS*, 297, L23
 Kodama, T., & Arimoto, Y. 1997, *A&A*, 320, 41
 Kuntschner, H. 2000, *MNRAS*, 315, 184
 Larson, R. B. 1974, *MNRAS*, 166, 585
 Michard, R. 1982, *A&AS*, 49, 591
 Schlegel, D. J., Finkbeiner, D. P., & Davis, M. 1998, *AJ*, 115, 525
 Terlevich, A., Kuntschner, H., Bower, R. G., Caldwell, N., & Sharples, R. 1999, *MNRAS*, 310, 445
 Trager, S., Faber, S., Worthey, G., & González, J. 2000a, *AJ*, 119, 1645
 ———. 2000b, *AJ*, 120, 165
 Vazdekis, A. 1999, *ApJ*, 513, 224
 Vazdekis, A., & Arimoto, N. 1999, *ApJ*, 525, 144
 Vazdekis, A., Casuso, E., Peletier, R. F., & Beckman, J. E. 1996, *ApJS*, 106, 307
 Vazdekis, A., Peletier, R. F., Beckman, J. E., & Casuso, E. 1997, *ApJS*, 111, 203
 Visvanathan, N., & Sandage, A. 1977, *ApJ*, 216, 214
 Worthey, G. 1994, *ApJS*, 95, 107
 ———. 1998, *PASP*, 110, 888
 Worthey, G., Faber, S. M., & González, J. J. 1992, *ApJ*, 398, 69
 Worthey, G., Faber, S. M., González, J., & Burstein, D. 1994, *ApJS*, 94, 687
 Worthey, G., & Ottaviani, D. L. 1997, *ApJS*, 111, 377